Pergamon

Chemosphere, Vol. 39, No. 1, pp. 55-70, 1999

0045-6535/99/ $ - see front matter

PII: S0045-6535(98)00588-8

MODELING AN OZONE BUBBLE COLUMN FOR PREDICTING ITS DISINFECTION EFFICIENCY AND CONTROL OF DBP FORMATION

P.-C. Chiang[1], Y.-W. Ko*[1], C.-H. Liang[1] and E.-E. Chang[2]

[1] Graduate Institute of Environmental Engineering, National Taiwan University, 71, Chou-Shan Rd., Taipei 106, Taiwan.

[2] Department of Analytical Chemistry, Taipei Medical College, Taipei 107, Taiwan.

(Received in Germany 11 September 1998; accepted 27 October 1998)

ABSTRACT

The prediction models describing the disinfection efficiency, the formation of aldehydes and the control of DBPs in the ozone bubble column were developed through a systematic approach. At low applied ozone doses, the predicted Ct values increased slightly with increasing gas flow rate. As the applied ozone dose increased, the influence of the gas flow rate on the Ct parameters became more apparent. The aldehyde formation increased to a maximum value when the ozone doses increased from 0.2 to 1.1 mg O_3/mg TOC; whereas a further increase of the ozone dose to 1.8 mg O_3/mg TOC decreased the aldehyde concentrations. The concentration profiles of aldehyde and DBP in the ozone bubble column were modeled at the different ozone dosages and compared with the experimental data. The utilization of a two-step reaction mechanism predicted the aldehyde formation reasonably well. Furthermore, the relationship between the optimization of ozone dosages and the disinfection efficiency, aldehyde formation and control of DBPs was discussed.

INTRODUCTION

There is an increasing use of ozone in drinking water treatment for the purpose of eliminating bacteria, viruses, cysts, as well as organic compounds, especially, the precursors of disinfection by-products (DBPs). The performance of the ozone disinfection processes is evaluated by the residual ozone and contact time. Therefore, factors such as the efficiency of gas-liquid contact, chemical reactivity of the raw water towards ozone, susceptibility of microorganisms and hydrodynamic characteristics of the contactor can influence the disinfection performance of an ozonation process [1,2]. In water treatment practices, it is therefore necessary

to adjust the operating conditions as to achieve the desired degree of inactivation. There are numerous research devoting to evaluating the hydraulic performance and to establishing the Ct value under various operating conditions, with C being the disinfectant concentration and t being the contact time in the reactor [3-8].

Several researchers have shown that ozonation prior to chlorination can lower the formation potential of THM (trihalomethanes) (THMFP) and HAA (haloacetic acid) (HAAFP) [9-11]. In addition, aldehyde has been identified as one of the ozonation by-products of great concern. Aldehydes can be related to possible adverse health effects and are highly biodegradable, which may lead to increasing bacterial populations in distribution systems [12-15]. Some investigators have shown that the aldehyde production increases with the increasing of ozone dose and ozonation time [16-17]; whereas the others reported that a further increase of ozonation time would reduce the aldehyde formation [13,18]. Therefore, it is necessary to maintain a balance relationship between the formation of chlorination by-products and the production of aldehydes during ozonation.

In our previous studies, the model balancing microbial safety and THM formation during chlorination [19], and the relationship between DBP and aldehyde formation in a agitation reactor [18] have been investigated, respectively. This paper presents the predictive models describing the disinfection efficiency, the formation of aldehydes and the control of DBPs during ozonation. An ozone bubble column was used. The systematic approach began with the tracer testing, as to obtain the hydrodynamic characteristics of the column. The concentration profiles of residual ozone in the water column were then developed and the Ct values were calculated as to measure disinfection efficiency. The concentration profiles of aldehyde and DBP were modeled at the different ozone dosages and compared with the experimental data. Furthermore, the relationship between the optimization of ozone dosage and the disinfection efficiency, aldehyde formation and control of DBPs was discussed.

MATERIAL AND METHODS

Ozone Bubble Column Figure 1 shows the schematic diagram of the ozone bubble column. The glass column, 2.25-m high and 12.5-cm diameter, was operated in the counter-current mode with water flowing downward and gas flowing upward. Ozone gas and water were both introduced continuously into the contactor. The water column depth used in the study was 1.80 m. Ozone was generated using pure oxygen with a Sumitomo SG-01A generator. The ozonated gas stream was introduced into the contactor through a ceramic diffuser located at 10 cm from the bottom of the contactor.

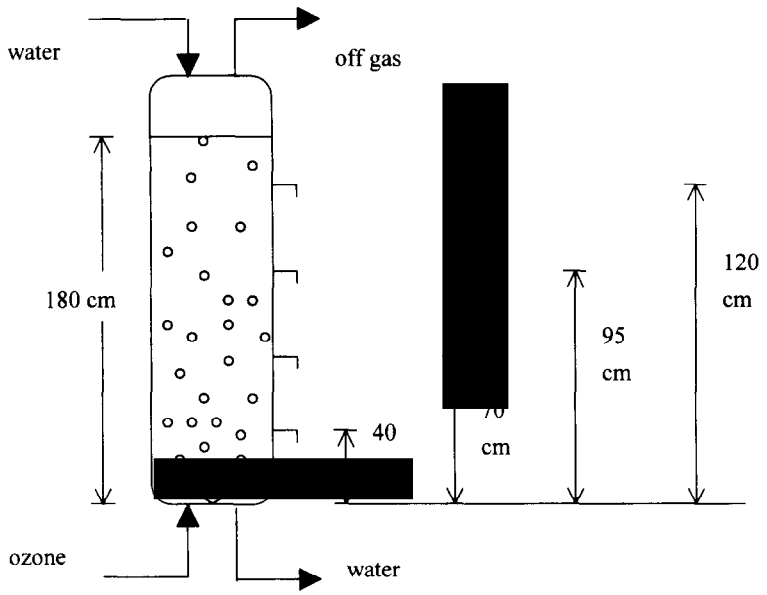

Figure 1. Schematic diagram of the ozone bubble column.

Tracer Test The tracer tests were conducted at various gas and water flow rates to characterize the hydrodynamic behavior of the contactor. Twelve tracer experiments were performed using only oxygen as surrogate gas. Water and gas flow rates were maintained at the range of 1.0~5.0 and 0.5~5.0 L/min, respectively. The water column was maintained constant at a height of 1.80 m. The water and oxygen gas flows were started, and the contactor was allowed to stabilize for one hour. Subsequently, a pulse-dose method was used wherein an instantaneous dose of concentrated NaCl solution (100000 mg/L) was injected into the inlet of the column. Samples were collected at discrete time intervals to determine the concentration distribution. NaCl concentration was determined with a conductometric probe.

Ozonation Test A total of four ozonation tests were performed with raw water collected at the Chang-Hsin Waterworks, Taipei, Taiwan, and spiked with commercial humic acid (Aldrich). The TOC concentration was about 7.0 mg/L. The gas and water flow rates were maintained constant at 0.5 and 2.0 L/min, respectively. The applied ozone dosage ranged from 0.2 to 1.8 mg O_3/mg TOC. Sample taps were installed at heights of 40, 70, 95 and 120 cm from the bottom of the contactor for sample collecting and the determination of aldehyde and DBP concentrations.

Analytical Methods Dissolved ozone concentrations were analyzed by the indigo method [20]. The TOC (O.I.C. Model 700) analysis was done by the UV-persulfate technique using the infrared carbon dioxide analyzer and calibrated with the potassium hydrogen phthalate standard.

Aldehydes, including formaldehyde, acetaldehyde, glyoxal and methyl glyoxal, were analyzed using the

method described by Sclimenti *et al.* [21]. O-(2,3,4,5,6-pentafluorobenzyl)-hydroxylamine hydrochloride (PFBOA·HCl) reacts with carbonyl compounds in aqueous solution to form the corresponding oximes. Derivatives were then extracted with n-hexane and analyzed using GC (HP 5890) equipped with a fused silica capillary column (DB-5, 30m * 0.25mm ID, 1.0 μ m film thickness) and an electron capture detector (ECD).

THMFP and HAAFP were measured after a 7-day incubation period following the introduction of sodium hypochlorite stock solution and phosphate buffer (pH 7.0). The applied chlorine concentration was about 45 mg/L, which was determined from the preliminary studies and would provide a free residual chlorine of at least 3 mg/L at the end of the incubation period. The analysis of residual chlorine was performed using the DPD (N,N-diethyl-p-phenylene-diamine) ferrous titration method.

THM was extracted with n-pentane. The extract was then analyzed using GC with a fused silica capillary column (same as described above) and an ECD. A microextraction procedure (extracting with methyl tert-butyl ether, esterifying with diazomethane) was used to analyze HAA, in accordance with *Standard Methods* [22]. The esterified extract was analyzed using GC with a fused silica capillary column (same as described above) and an ECD.

RESULTS AND DISCUSSION

Ozone Disinfection Performance The performance of the ozone disinfection processes is evaluated in terms of the residual ozone and the contact time. Table 1 summarizes results of tracer tests. When water flow rate was at a fixed level, d (dimensionless dispersion number) values generally decreased with the decrease of gas flow rate. This implies that the mixing condition approached that of an ideal plug flow as the gas flow rate decreased. According to Doquang *et al.* [6], the ratio of MRT (mean retention time) to HRT (hydraulic retention time) was considered as an index reflecting the percentage of stagnant space in the bubble column. At a water flow rate of 1.0 L/min, the MRT/HRT ratios were about 0.6 to 0.7, indicating a possible presence of the stagnant region of 30 to 40 % of the column volume. At water flow rate of 2.0 L/min, the MRT/HRT ratios were higher than those at 1.0 or 5.0 L/min and stayed around 1.0, except for the case of 0.5 L/min gas flow rate. It was thus speculated that the optimum hydraulic condition in the bubble column was controlled at a water flow rate of 2.0 L/min. Consequently, it was applied to the subsequent experiments.

It has also been suggested that the t_{10}/HRT (t_{10} is the time required for 10 % of the total tracer mass to leave the contactor) is measurement of the degree of short-circuiting in the contactor [3,23]. As seen in Table 1, t_{10}/HRT values decreased as gas flow rate increased while the water flow rates were kept constant. It means that hydraulic efficiency of the bubble column can be enhanced with the decrease of gas flow rate. Based on the N(CSTR) parameters (number of equivalent CSTR in series), it indicates that the mixing condition

inside the contactor did not change much under these operating conditions.

Table 1. Summary of tracer test operating conditions and results*

Q_G (L/min)	Q_L (L/min)	HRT (min)	MRT (min)	t_{10} (min)	MRT /HRT	t_{10}/HRT	d	N(CSTR)	Pe
0.5	1.0	21.48	13.53	2.28	0.63	0.11	0.3800	2	2.6316
1.0	1.0	21.48	15.38	2.02	0.72	0.09	0.3487	2	2.8678
2.0	1.0	21.48	14.05	1.81	0.65	0.08	0.4164	2	2.4015
5.0	1.0	21.48	13.70	1.49	0.64	0.07	0.4440	2	2.2523
0.5	2.0	10.74	14.15	3.25	1.32	0.30	0.2908	2	3.4388
1.0	2.0	10.74	11.62	2.55	1.08	0.24	0.4325	2	2.3121
2.0	2.0	10.74	11.40	1.61	1.06	0.15	0.4677	2	2.1381
5.0	2.0	10.74	11.90	1.55	1.11	0.14	0.4966	2	2.0137
0.5	5.0	4.30	3.51	1.17	0.82	0.27	0.1886	3	5.3022
1.0	5.0	4.30	3.19	0.93	0.74	0.22	0.2297	3	4.3535
2.0	5.0	4.30	3.10	0.83	0.72	0.19	0.2575	3	3.8835
5.0	5.0	4.30	3.16	0.69	0.73	0.16	0.3041	2	3.2884

*: HRT, hydraulic retention time; MRT, mean retention time; t_{10}, time for 10 % of total tracer mass to exit the contactor, in min; d, dimensionless dispersion number; N(CSTR), number of equivalent CSTR in series; Pe, Peclet Number.

The dispersion numbers and t_{10} values shown in Table 1 were correlated to the operation conditions by multiple regression analysis (SYSTAT 5.0). Equation (1) and (2) showed the relationship obtained:

$$d = \frac{1}{Pe} = 0.454(Re_G)^{0.163}(Re_L)^{-0.257}, \qquad R^2 = 0.660 \tag{1}$$

$$\frac{t_{10}}{HRT} = 0.121(Re_G)^{-0.288}(Re_L)^{0.368}, \qquad R^2 = 0.673 \tag{2}$$

where Re_G is the gas-phase Reynolds number,

Re_L is the liquid-phase Reynolds number.

Equation (1) suggests that dispersion number increased as the gas flow rate increased and the water flow rate decreased. Furthermore, the water flow rate plays a much significant role since the absolute value of the exponential term in the water flow rate in equation (1) is relatively greater than that in the gas flow rate.

The dissolved ozone concentration profile in the contactor was developed based on the assumptions and dispersion model used by Marinas *et al.* [4], and the hydrodynamic information obtained above. The numerical technique, including the finite difference and Newton-Raphson methods, were applied to model solution. Figure 2 and 3 show the simulation results of the ozone concentration profile model, under various gas and water flow rates. Increasing the gas flow rate resulted in the enhancement of influent ozone dosage, dispersion number (or the decrease of Peclet number) and bubble diameter, while the first factor is the dominant one. The effect of the water flow rate on the dissolved ozone concentration profiles is shown in

Figure 3. The increase of the water flow rate not only led to decreasing dispersion number, increasing a (interfacial area per unit volume) value; but also caused the flow behavior to approach that of an ideal plug flow pattern. Consequently the chemical reaction in the bubble column was more efficient under higher water flow rate; thereby the dissolved ozone concentrations were smaller near the top of the contactor.

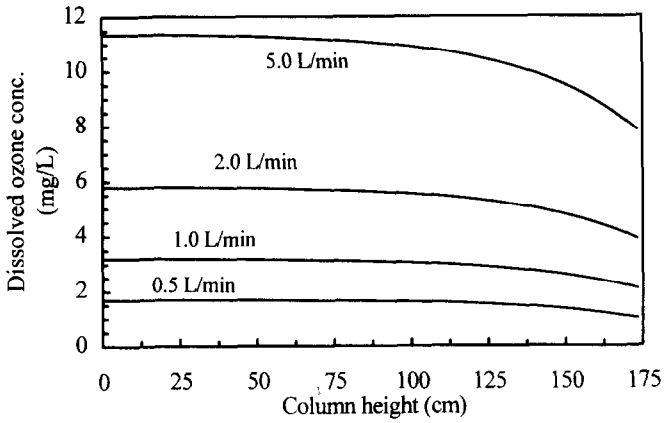

Figure 2. Effect of the gas flow rate on the dissolved ozone concentration profiles in the bubble column (water flow rate= 2.0 L/min, applied gaseous ozone concentration= 18.4 mg/L).

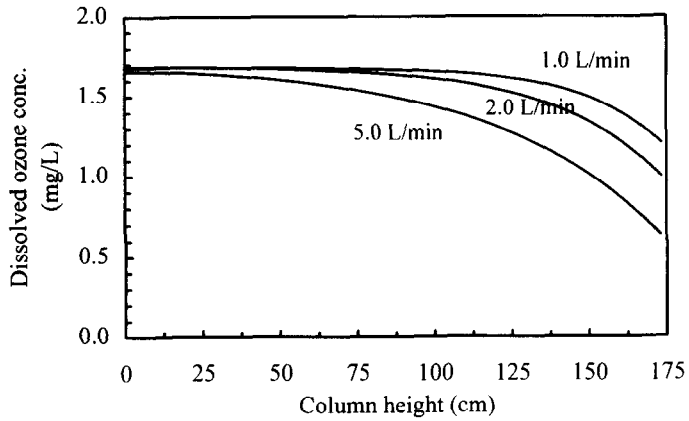

Figure 3. Effect of the water flow rate on the dissolved ozone concentration profiles in the bubble column (gas flow rate= 0.5 L/min, applied gaseous ozone concentration= 18.4 mg/L).

Figure 4 shows the predicted concentration profile of residual ozone in water with corresponding experimental data. In general the model predicts the dissolved ozone concentration well, with the exception of the ozone concentrations near the top and the bottom of the contactor. Since the water and ozone gas injection points are located at the bottom and the top of the contactor, it is speculated that the mixing conditions in these regions are beyond the prediction by the dispersion model.

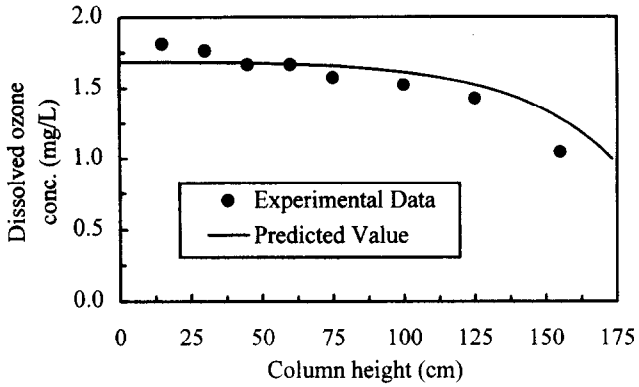

Figure 4. Comparison of the predicted dissolved ozone concentration profile and experimental data in the bubble column (water flow rate= 2.0 L/min, gas flow rate= 0.5 L/min, applied gaseous ozone concentration= 18.4 mg/L).

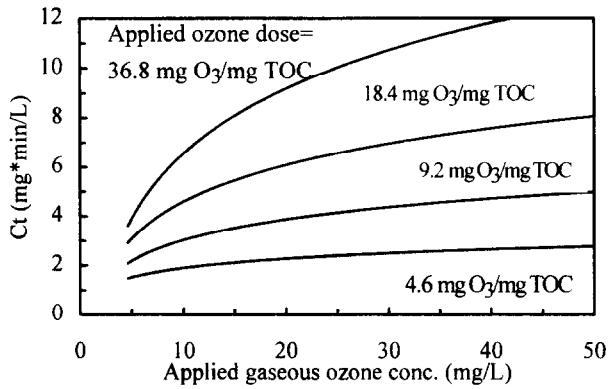

Figure 5. Predicted Ct values dependence on the applied gaseous ozone concentration and applied ozone dose.

Knowing the t_{10} values and dissolved ozone concentration profile along the contactor, the Ct values could be estimated. The average ozone concentration was used for C by means of integrating the dissolved ozone concentrations over the bubble column. Figure 5 shows the dependence of Ct value on the applied ozone dose under various gas flow rates. At the low applied ozone doses, the predicted Ct values increased slightly with increasing gas flow rates. As the applied ozone dose increased, the influence of the gas flow rate on the Ct parameters became more apparent. Figure 5 can provide the baseline information of critical applied ozone dose for design and operation of the ozone bubble column for disinfection requirement. The higher the applied gaseous ozone concentration, the lower the applied ozone dosage (i.e. the lower the gas flow rate) needed to achieve the same level of disinfection efficiency. When ozone demand of the system and the

applied ozone dosage are low, the enhancement of the gaseous ozone concentration cannot significantly increase the Ct credit and the most efficient dosage of the applied ozone can then be determined through the use of Figure 5. On the other hand, at a fixed applied gaseous ozone concentration, the disinfection efficiency and Ct values increased with the increase of the applied ozone dosage (or the gas flow rate).

Modelization of Aldehyde Concentration Profile Aldehyde formation was examined at the different column heights and ozone dosages, aiming at the development of aldehyde concentration profile model in the bubble column. Table 2 shows the measured formaldehyde, glyoxal and methyl glyoxal concentrations along the bubble column. Some investigators have shown that the aldehyde production increased with the increase of ozone dosage and ozonation time [16,17]. Since the contactor was operated in the counter-current mode, water flowed downwards and gas flowed upwards, the contact time between ozone and organic compounds increased as the height decreased. Therefore the increase of aldehyde formation with the decrease of height could be observed from Table 2.

When the ozone doses increased from 0.2 to 1.1 mg O_3/mg TOC, the generated aldehydes increased accordingly; whereas a further increase in ozone dose to 1.8 mg O_3/mg TOC decreases the aldehyde concentrations. Results of previous research demonstrated that aldehyde production first increased then decreased with increasing ozonation time in the semi-batch operation, as aldehydes may decompose readily even though considerable quantities were produced [18]. In the continuous-type bubble column, the dissolved ozone concentration profiles were at the steady state and were independent of time. Aldehyde production increased to a maximum value then decreased with further increase in ozone dosages rather than the ozonation time in the case of semi-batch operation.

In batch reaction, the formation of aldehyde can be expressed by the following simple equations:

$$\mathrm{TOC} + \mathrm{O_3} \xrightarrow{k_1} \mathrm{Ald} \tag{3}$$

$$\mathrm{Ald} + \mathrm{O_3} \xrightarrow{k_2} \mathrm{P} \tag{4}$$

where TOC designates the total sum of all of the possible precursors or functional groups which would react with ozone to form aldehydes, and P represents all of the products formed by the reaction of aldehydes and ozone. Equations (3) and (4) are the short-hand way of describing a whole series of reactions. Assuming a first-order reaction with respect to the individual reactant, the formation rate of aldehyde can be expressed by the following:

$$\frac{d[\mathrm{Ald}]}{dt} = k_1[\mathrm{TOC}][\mathrm{O_3}] - k_2[\mathrm{O_3}][\mathrm{Ald}] \tag{5}$$

The reaction rate of TOC can be assumed as below:

$$\frac{d[\mathrm{TOC}]}{dt} = -k_3[\mathrm{TOC}] \tag{6}$$

Table 2. Experimental data and predicted aldehyde concentration at the different column heights and ozone dosages*

Ozone dose= 0.2 mg O_3/mg TOC						
Column height (cm)	Formaldehyde (μg/L)		Glyoxal (μg/L)		Methyl Glyoxal (μg/L)	
	Experimental data	Predicted value	Experimental data	Predicted value	Experimental data	Predicted value
120	14.7	15.6	6.9	6.2	5.4	4.5
95	19.1	17.0	7.5	6.8	5.4	5.2
70	18.8	17.9	7.3	7.1	5.3	5.6
40	17.0	18.6	8.3	7.4	6.4	5.9
0	20.6	19.7	8.3	7.9	7.1	6.4
Ozone dose= 0.5 mg O_3/mg TOC						
Column height (cm)	Formaldehyde (μg/L)		Glyoxal (μg/L)		Methyl Glyoxal (μg/L)	
	Experimental data	Predicted value	Experimental data	Predicted value	Experimental data	Predicted value
120	18.7	18.1	7.3	8.3	8.5	8.9
95	20.0	19.8	7.5	9.1	9.2	10.2
70	18.0	20.8	7.8	9.6	10.1	11.0
40	22.5	21.7	8.9	10.0	11.3	11.6
0	21.6	22.9	10.3	11.0	12.0	12.4
Ozone dose = 1.1 mg O_3/mg TOC						
Column height (cm)	Formaldehyde (μg/L)		Glyoxal (μg/L)		Methyl Glyoxal (μg/L)	
	Experimental data	Predicted value	Experimental data	Predicted value	Experimental data	Predicted value
120	21.0	19.0	11.5	9.8	10.8	10.3
95	20.0	20.7	11.8	10.7	12.0	11.8
70	19.5	21.8	12.2	11.3	14.6	12.7
40	25.3	22.6	13.6	11.7	14.1	13.4
0	24.7	23.7	14.6	12.7	14.4	14.1
Ozone dose = 1.8 mg O_3/mg TOC						
Column height (cm)	Formaldehyde (μg/L)		Glyoxal (μg/L)		Methyl Glyoxal (μg/L)	
	Experimental data	Predicted value	Experimental data	Predicted value	Experimental data	Predicted value
120	14.1	15.1	7.3	8.2	6.9	7.2
95	16.3	16.5	8.5	9.0	7.9	8.2
70	14.7	17.3	8.5	9.5	7.9	8.8
40	20.7	18.0	9.6	9.9	8.5	9.3
0	16.7	18.6	8.9	10.4	8.6	9.7

*: water flow rate= 2 L/min, gas flow rate= 0.5 L/min.

Equations (5) and (6) can be integrated under given initial and boundary conditions. Since the change of dissolved ozone concentration is much smaller than that of the degradation of TOC, it is reasonable to assume that $[O_3]$ remains constant. Furthermore, under the following initial conditions:

$$[Ald] = 0, \text{ at } t = 0 \tag{7}$$

and

$$[TOC] = [TOC]_0, \text{ at } t = 0 \tag{8}$$

The integrated forms of Equations (5) and (6) are

$$[TOC]=[TOC]_0 e^{-k_3 t} \tag{9}$$

$$[Ald]=\frac{K_1'}{k_2'-k_3}\left(e^{-k_3 t}-e^{-k_2' t}\right) \tag{10}$$

where

$$K_1' = k_1[O_3][TOC]_0 \tag{11}$$

$$k_2' = k_2[O_3] \tag{12}$$

As for the steady state operation in the bubble column, the aldehyde formation is no longer a function of the ozonation time. Results also indicated that the column height and ozone dosage can also affect the aldehyde concentration. Consequently these two parameters should be incorporated into Equation (10). Aldehyde formation is proportional to the column height. On the other hand, the role of ozone dosage in the continuous mode is similar to that of ozonation time in the semi-batch mode. Besides, $[O_3]$ is directly influenced by the ozone dosage, as discussed in the previous section. Therefore, equation (10) can be transformed into the following:

$$[Ald]=c_1 \times OD^{c_2} \times (180-L)^{c_3} \times \left(e^{-c_4 \times OD}-e^{-c_5 \times (OD)^2}\right) \tag{13}$$

where OD denotes ozone dose, in unit of mg O_3/mg TOC, L denotes the depth of water column (L= 180 - height), in unit of cm, c_1, c_2, c_3, c_4 and c_5 are constants to be determined.

For each aldehyde compound, substitution of 20 sets of experimental results into Equation (13) led to the prediction models for aldehyde formation, by the use of multiple regression analysis (SYSTAT 5.0). Table 3 shows the estimated parameters in Equation (13) (c_1 to c_5) for three aldehydes.

The predicted values of formaldehyde, glyoxal and methyl glyoxal from Equation (13) are shown in Table 2. In comparison with the measured data, the model can described the aldehyde concentration profile and trend reasonably well. That is, aldehyde production increased to a maximum value when the ozone doses increased from 0.2 to 1.1 mg O_3/mg TOC; whereas a further increase in the ozone dose to 1.8 mg O_3/mg TOC decreased the aldehyde concentrations.

Table 3. Parameter estimates for equation (13)

Species	c_1	c_2	c_3	c_4	c_5
Formaldehyde	14.221	-1.442	0.194	-0.110	0.695
Glyoxal	5.908	-1.289	0.237	-0.095	0.761
Methyl Glyoxal	5.370	-1.237	0.270	0.031	1.188

Prediction of the Elimination of DBP Precursors by Ozonation In this study, due to the absence of bromide ion, the major species found in THM and HAA groups were chloroform, TCAA (trichloroacetic acid) and DCAA (dichloroacetic acid). Figure 6, 7 and 8 show the reduction ratio of chloroform formation potential, TCAAFP and DCAAFP along the bubble column under various ozone dosages, respectively. Usually DBP concentrations decreased with increasing ozone dosage, indicating the effectiveness of ozonation in the control of DBPFP. Additionally, DBPFP formation gradually increased along the height of the column, though the increase was not significant.

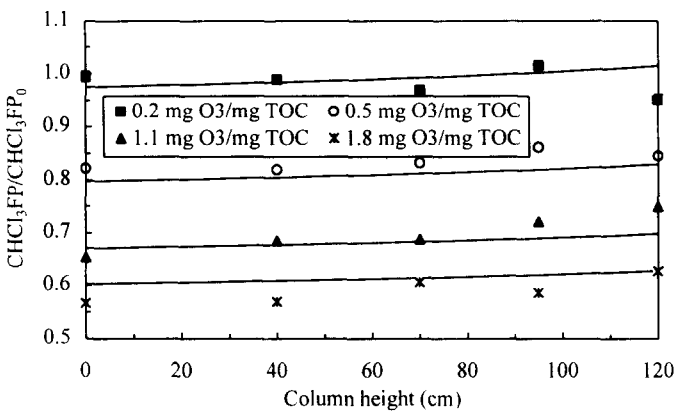

Figure 6. Effect of applied ozone dosage on the $CHCl_3FP$ profile along the bubble column (water flow rate= 2.0 L/min, gas flow rate= 0.5 L/min).

Table 4 summarizes the correlations between UV254, TOC, $CHCl_3FP$, TCAAFP and DCAAFP and the column height and applied ozone dosages. Among these water quality indicators, the R^2 value of TOC is the lowest. Since the total oxidation of organic matter is not the main treatment objective for ozonation, the reduction of TOC in the contactor is limited. Further, the exponential term of the ozone dosage is higher than that of the column height for all of the regression correlations. It is concluded that the effect of ozone dosage on the reduction of organic precursors and DBPFP is more prominent than that of the column height.

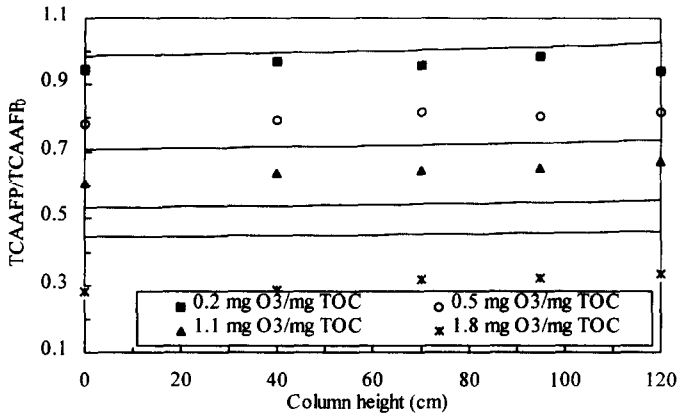

Figure 7. Effect of applied ozone dosage on the TCAAFP profile along the bubble column (water flow rate= 2.0 L/min, gas flow rate= 0.5 L/min).

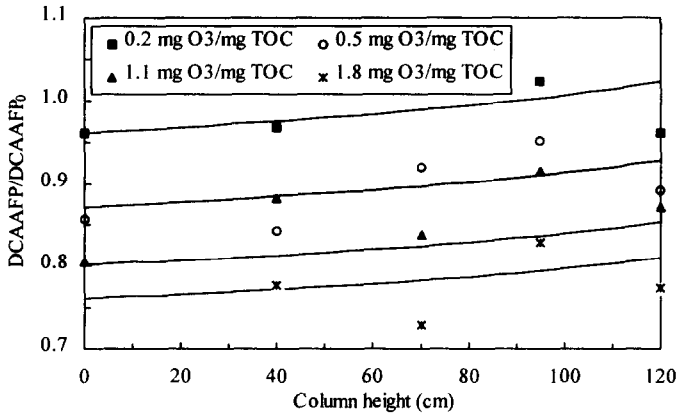

Figure 8. Effect of applied ozone dosage on the DCAAFP profile along the bubble column (water flow rate= 2.0 L/min, gas flow rate= 0.5 L/min).

From the above discussion, effects of ozonation on the trends of aldehyde formation and on the control of DBPFP are quite different. Although the current regulatory standards only focus on THM concentration, HAA and aldehyde have drawn more attention for their potentially adverse health effects. Therefore when it comes to ozonation, not only the removal of DBP precursors but also its by-products produced ought to be taken into account. Figure 9 shows the relationship among the applied ozone dose, aldehyde formation and DBPFP concentrations at the exit of bubble column. Table 4 shows the empirical formula for predicting the reduction ratio of various organic compounds in the column. Figure 9 shows the simulation results for the Taipei raw water at THMFP= 139.9 μ g/L and HAAFP= 120.7 μ g/L. The utilities of Figure 9 are obvious. For instance, in order to ensure THM concentration be kept within the drinking water quality regulations,

minimum ozone dosage required is about 0.7 mg O_3/mg TOC. However, considering the aldehyde produced under the dosage or the more stringent water quality standards in the future, it relies on the enhancement of treatment performance of the subsequent unit operations.

Table 4. Regression equations of the concentrations of organic precursors and DBPFP *

Regression equation	R^2 (N)
$UV254=0.149\times(180-L)^{-0.116}\times(OD)^{-0.609}$	0.989 (20)
$UV254/UV254_0=0.440\times(180-L)^{-0.111}\times(OD)^{-0.643}$	0.990 (20)
$TOC=6.687\times(180-L)^{-0.051}\times(OD)^{-0.089}$	0.623 (20)
$TOC/TOC_0=1.036\times(180-L)^{-0.051}\times(OD)^{-0.091}$	0.534 (20)
$CHCl_3FP=627.581\times(180-L)^{-0.035}\times(OD)^{-0.223}$	0.879 (20)
$CHCl_3FP/CHCl_3FP_0=0.826\times(180-L)^{-0.036}\times(OD)^{-0.219}$	0.964 (20)
$TCAAFP=398.060\times(180-L)^{-0.039}\times(OD)^{-0.306}$	0.691 (20)
$TCAAFP/TCAAFP_0=0.664\times(180-L)^{-0.036}\times(OD)^{-0.361}$	0.825 (20)
$DCAAFP=279.873\times(180-L)^{-0.053}\times(OD)^{-0.195}$	0.942 (20)
$DCAAFP/DCAAFP_0=1.089\times(180-L)^{-0.057}\times(OD)^{-0.106}$	0.793 (20)

*: OD= ozone dose, mg O_3/mg TOC; L= the depth of water column (= 180 - height), cm; UV254 is in unit of cm^{-1}; TOC is in unit of mg/L; $CHCl_3FP$, TCAAFP and DCAAFP are in unit of μ g/L.

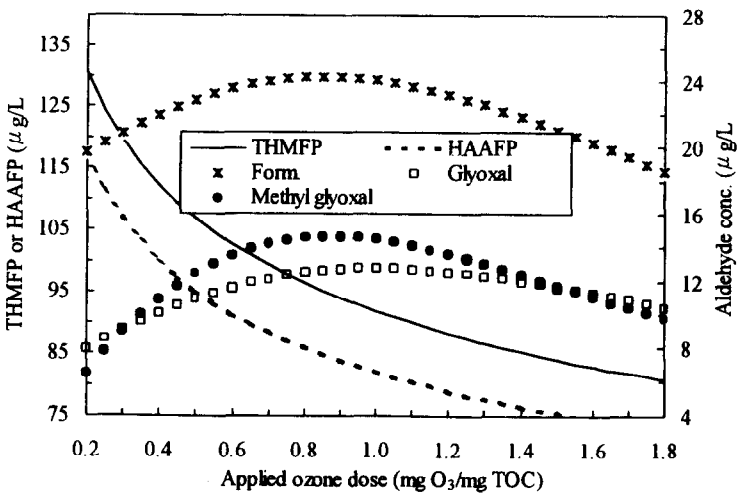

Figure 9. Effect of the applied ozone dose on the aldehyde formation and DBPFP concentrations at the exit of bubble column (water flow rate= 2.0 L/min; gas flow rate= 0.5 L/min).

CONCLUSIONS

The prediction models describing the disinfection efficiency, the formation of aldehydes and the control of DBPs in the ozone bubble column were developed through a systematic approach. The concentration profile of residual ozone was first established and the disinfection performance of the bubble column was evaluated. At the low applied ozone doses, the predicted Ct values increased slightly with increasing gas flow rates. As the applied ozone dose increased, the influence of the applied gaseous ozone concentration on the Ct parameters became more apparent.

Based on the selected operation conditions, i.e. the water and gas flow rate, the formation of aldehydes and DBPs was modeled and compared with the experimental data. As for aldehyde formation, it increased to a maximum value when the ozone doses increased from 0.2 to 1.1 mg O_3/mg TOC; whereas a further increase of the ozone dose to 1.8 mg O_3/mg TOC decreased the aldehyde concentrations. The utilization of a two-step reaction mechanism predicted the aldehyde formation in the bubble column reasonably well.

DBP concentrations decreased with increasing applied ozone dosage, indicating the effectiveness of the ozonation process for the control of DBPFP. DBPFP formation gradually increased as the column height increased, though the dependence was not significant. The regression equations for UV254, TOC, $CHCl_3FP$, TCAAFP and DCAAFP concentrations at the various column heights and applied ozone dosages were established.

The relationship among the applied ozone dose, aldehyde formation and DBPFP concentrations at the exit of bubble column was examined. The trade-off among different species and the optimum ozone dosage can be determined to achieve disinfection and oxidation requirement. For instance, in order to ensure THM concentration being within the drinking water quality regulations, the minimum ozone dosage required for the Taipei raw water at THMFP= 139.9 μ g/L and HAAFP= 120.7 μ g/L is about 0.7 mg O_3/mg TOC.

ACKNOWLEDGMENTS

The authors are grateful for the financial support of the Environmental Protection Agency of Taiwan, Division of Toxicant Control, with the grant: EPA-87-E3J1-09-01, and assistance of Chang-Hsin water treatment plant, Taipei, Taiwan. Valuable discussion with Prof. C. P. Huang from the Department of Civil Engineering, University of Delaware is highly appreciated.

REFERENCES

1. S. Farooq, R. S. Engelbrecht and E. S. K. Chian, Basic concepts in disinfection with ozone, *J. WPCF* **49**, 1818-1831 (1979).

2. D. W. Smith and H. Zhou, Theoretical analysis of ozone disinfection performance in a bubble column, *Ozone Sci. & Engrg.* **16**, 429-441 (1994).

3. B. Langlais, D. A. Reckhow and D. B. Brink, *Ozone in Water Treatment- Application and Engineering*, Lewis Publishers, Michigan (1991).

4. B. J. Marinas, S. Liang, and E. M. Aieta, Modeling hydrodynamics and ozone residual distribution in a pilot-scale ozone bubble-diffuser contactor, *J. Amer. Water Works Assoc.* **85**, 90-99 (1993).

5. J. F. Holmes, D. J. Rodman and F. H. Ehrlich, Optimisation of ozone processes for disinfection and advanced oxidation of drinking waters in the UK, USA and the Netherlands, *Proceedings of International Ozone Association Regional Conference*, pp. 81-94. Zurich (1994).

6. Z. Doquang, C. Ramirez-Cortina and M. Roustan, Modeling of the flow pattern in ozonation chambers contactor by residence time distribution studies and by computational fluid dynamics approach, *Proceedings of the 12th International Ozone Association World Congress*, Vol. 2, pp. 215-226. Lille, France (1995), .

7. J. Murrer, J. Gunstead and S. Lo, The development of an ozone contact tank simulation model, *Ozone Sci. & Engrg.* **17**, 607-617 (1995).

8. A. Reading and J. Bell, Inactivation of cryptosporidium oocysts in surface waters using ozonation, *Proceedings of the 12th International Ozone Association World Congress*, Vol. 1, pp. 467-476. Lille, France (1995).

9. J. G. Jacangelo, N. L. Patania, K. M. Reagau, E. M, Aieta, S. W. Krasner and M. J. McGuire, Ozonation: assessing its role in the formation and control of disinfection by-products, *J. Amer. Water Works Assoc.* **81**, (1989).

10. G. L. Amy, L. Tan and M. K. Davis, The effects of ozonation and activated carbon adsorption on trihalomethane speciation, *Wat. Res.* **25**, 191-202 (1991).

11. E.-E. Chang and P.-C. Chiang, Assessment of DBPs removal by ozonation coupled with adsorption, *Toxicol. & Envir. Chem.* **52**, 249-262 (1995).

12. P. C. Singer, Assessing ozonation research needs in water treatment, *J. Amer. Water Works Assoc.* **82**, 78-88 (1989).

13. R. Gracia, J. L. Aragues and J. L. Ovelleiro, Study of the catalytic ozonation of humic substances in water and their ozonation byproducts, *Ozone Sci. & Engrg.* **18**, 195-208 (1996).

14. H. S. Weinberg and W. H. Glaze, An overview of ozonation disinfection by-products. In *Disinfection By-Products in Water Treatment* (Edited by R. A. Minear and G. L. Amy), Chap. 7. Lewis Publishers, Boca Raton, Florida (1996).

15. H. S. Weinberg and W. H. Glaze, A unified approach to the analysis of polar organic by-products of oxidation in aqueous matrices, *Wat. Res.* **31**, 1555-1572 (1997).

16. W. H. Glaze, M. Koga and D. Cancilla, Ozonation byproducts: 2 improvement of an aqueous-phase derivatization method for the detection of formaldehyde and other carbonyl compounds formed by the ozonation of drinking water, *Environ. Sci. Technol.* **23**, 838-847 (1989).

17. H. Yamada and I. Somiya, The determination of carbonyl compounds in ozonated water by the PFBOA method, *Ozone Sci. & Engrg.* **17**, 53-69 (1989).

18. Y.-W. Ko, P.-C. Chiang and E.-E. Chang, Ozonation of p-hydroxybenzoic acid solution, accepted in *Ozone Sci. & Engrg.* (1998).

19. P.-C. Chiang, E.-E. Chang, Y.-W. Ko and J.-C. Lou, Balancing disinfection efficiency and THM formation during chlorination: theoretical considerations, *Canadian J. Chem. Engrg.* **75**, 892-898 (1997).

20. H. Bader and J. Hoigne, Determination of ozone in water by the indigo method, *Wat. Res.* **15**, 449-456. (1981).

21. M. J. Sclimenti, S. W. Krasner, W. H. Glaze and H. S. Weinberg, Ozone disinfection by-products: optimization of the PFBHA derivatization method for the analysis of aldehydes, *Proceeding of Amer. Water Works Assoc. Water Quality Technology Conference*, San Diego (1990).

22. *Standard Method for the Examination of Water and Wastewater* (19th Edn), Prepared and published by APHA, AWWA, and WEF, Washington (1995).

23. D. J. Henry and E. M. Freeman, Finite element analysis and t_{10} optimization of ozone contactors, *Proceedings of the 12th International Ozone Association World Congress*, Vol. 2, pp. 201-214. Lille, France (1995).